Enzyme Catalysis

Deutsche Ausgabe: DOI: 10.1002/ange.201606223
Internationale Ausgabe: DOI: 10.1002/anie.201606223

3D Structure Determination of an Unstable Transient Enzyme Intermediate by Paramagnetic NMR Spectroscopy

*Jia-Liang Chen, Xiao Wang, Feng Yang, Chan Cao, Gottfried Otting, and Xun-Cheng Su**

Abstract: *Enzyme catalysis relies on conformational plasticity, but structural information on transient intermediates is difficult to obtain. We show that the three-dimensional (3D) structure of an unstable, low-abundance enzymatic intermediate can be determined by nuclear magnetic resonance (NMR) spectroscopy. The approach is demonstrated for Staphylococcus aureus sortase A (SrtA), which is an established drug target and biotechnological reagent. SrtA is a transpeptidase that converts an amide bond of a substrate peptide into a thioester. By measuring pseudocontact shifts (PCSs) generated by a site-specific cysteine-reactive paramagnetic tag that does not react with the active-site residue Cys184, a sufficient number of restraints were collected to determine the 3D structure of the unstable thioester intermediate of SrtA that is present only as a minor species under non-equilibrium conditions. The 3D structure reveals structural changes that protect the thioester intermediate against hydrolysis.*

Delineating conformational changes in enzymes at atomic resolution is required for a detailed understanding of their functions.[1,2] Different methods for the structural characterization of enzymes during chemical reaction have recently been developed.[1–3] Structure determination of unstable enzyme intermediates in solution, however, is still a challenge in view of the short lifetime and low abundance of these intermediates. Recent advances in NMR spectroscopy have made it possible to gain structural information on sparsely populated species present in equilibrium by using experiments such as relaxation dispersion, paramagnetic relaxation enhancement (PRE), pseudocontact shift (PCS), chemical exchange saturation transfer (CEST), and dark exchange saturation transfer (DEST) measurements.[4–7] Among these parameters, PCSs stand out for providing localization restraints for nuclear spins relative to the paramagnetic center that can be measured in minutes in sensitive heteronuclear single quantum coherence (HSQC) spectra.

Herein, we describe the use of PCSs to determine the 3D structure of the unstable transient thioester intermediate formed by *Staphylococcus aureus* Sortase A (SrtA) and a peptide substrate under non-equilibrium conditions. SrtA is an important enzyme in Gram-positive bacteria. It converts a backbone amide of a substrate peptide (the peptide bond between threonine and glycine in polypeptides containing the LPXTG motif, where X can be any amino acid) into a thioester with the active-site cysteine residue (Cys184).[8–11] SrtA is an established drug target[10] and is increasingly being used as a biotechnological tool for protein ligations.[12,13] 3D structures of SrtA have been determined by X-ray crystallography and NMR spectroscopy.[14,15] The structure of the disulfide-bond-linked intermediate analogue SrtA-LPAT* showed significantly different structural features to free SrtA or SrtA in a non-covalent complex with a peptide substrate.[16] While the occurrence of a SrtA thioester intermediate can be detected by mass spectrometry,[17,18] the 3D structure of this unstable intermediate has not been determined. Thioester complexes are intermediates in many enzyme reactions,[19] thus making techniques for their structural elucidation highly desirable.

We identified conditions under which SrtA (without the N-terminal 58 amino acids, which serve as a membrane anchor in full-length SrtA)[14] transiently displays resolved NMR resonances for the thioester intermediate formed between Cys184 of SrtA and the threonine residue of the substrate peptide QALPETG-NH_2, where the C-terminal amide serves as an uncharged protection group. The 3D structure of the intermediate was determined by measuring PCSs from new site-specifically attached paramagnetic lanthanide tags.

NMR signals for the thioester intermediate were identified by monitoring the reaction of SrtA with the substrate peptide QALPETG-NH_2 by ^{15}N-HSQC spectroscopy (Figures S1 and S2 in the Supporting Information). Many new weak cross-peaks appeared (Figure 1 a) in the spectrum of the mixture of SrtA, calcium, and peptide, and they decayed with a half-life of about 2.5 hours (Figure S2). A five-fold increase in the concentration of SrtA or peptide did not increase the population of the minor species, which was most highly populated at pH 6.4 (Figure S1). Mass spectrometry indicated that the new species was the thioester intermediate (Figure S1).[17,18] The intermediate could not be detected in the absence of calcium or in the presence of 1.0 mM tri-glycine peptide, which is known to act as a second substrate and resolve the thioester by forming a peptide bond with the bound first substrate (Figures S3–S5). The affinity of SrtA for the substrate and product peptide is very weak, as indicated by the conservation of chemical shifts of the main species (Figure 1 a), which corresponds to free SrtA, even in the presence of a 20-fold excess of substrate peptide and after

[*] Dr. J.-L. Chen, X. Wang, F. Yang, C. Cao, Prof. X.-C. Su
State Key Laboratory of Elemento-Organic Chemistry, Collaborative Innovation Center of Chemical Science and Engineering (Tianjin)
Nankai University, Tianjin 300071 (China)
E-mail: xunchengsu@nankai.edu.cn
Prof. G. Otting
Research School of Chemistry, Australian National University
Canberra, ACT 2601 (Australia)
Supporting information and the ORCID identification number(s) for the author(s) of this article can be found under http://dx.doi.org/10.1002/anie.201606223.

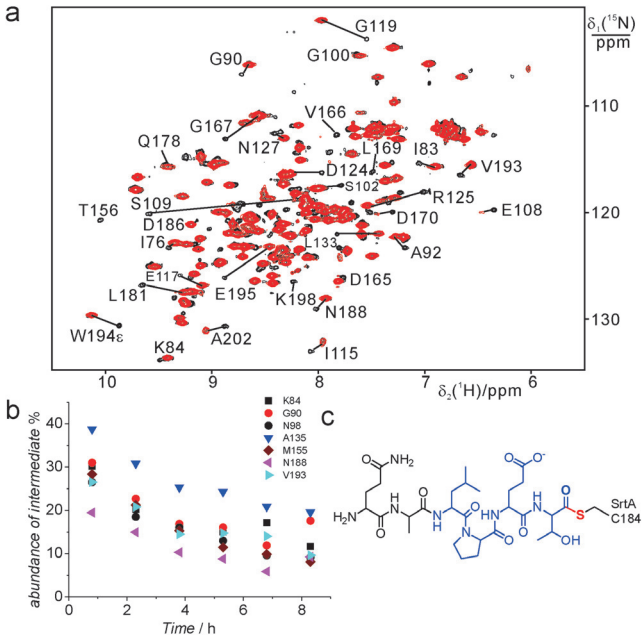

Figure 1. NMR detection of the SrtA thioester intermediate during hydrolysis of the substrate peptide. All ^{15}N-HSQC spectra were recorded in 0.1 mM solutions of uniformly ^{15}N-labeled SrtA in 20 mM MES buffer, pH 6.4, at 298 K in the presence of 1.0 mM $CaCl_2$. a) Superimposition of ^{15}N-HSQC spectra before (red) and after (black) mixing with 1.0 mM peptide QALPETG-NH_2. Corresponding cross-peaks of the thioester intermediate (minor species) and free SrtA (major species) from the same residues are connected by lines. b) Cross-peak heights of selected residues of the thioester intermediate relative to the sum of the cross-peak amplitudes of minor and major species, which provide an estimate of the population and decay rate of the thioester species. Cross-peak amplitudes varied between different residues due to different line widths in the minor and major species. c) Chemical structure of the thioester intermediate formed between SrtA and QALPETG-NH_2.

prolonged reaction times (Figures S3 and S5). There was no evidence for slow exchange between free SrtA and any non-covalent complex with the substrate or product peptide (Figure S5).

The lifetime of the thioester complex was too short and its concentration too low for NMR resonance assignments by standard 3D triple-resonance experiments (Figures S1 and S2). Therefore, we assigned the resonances by comparison with a stable disulfide-bonded analogue produced by ligating the peptide QALPECG-NH_2 to Cys184 of SrtA (Scheme S1).[20] This adduct displayed ^{15}N-HSQC cross-peaks with very similar chemical shifts as the SrtA–QALPET thioester complex with Ca^{2+}. The backbone resonances of the SrtA–QALPECG-NH_2 adduct were assigned based on a 3D NOESY-^{15}N-HSQC spectrum. Large differences in chemical shift between the SrtA–QALPECG-NH_2 adduct and the thioester intermediate were limited to amides near Cys184, reflecting the chemical difference between the disulfide and thioester bond linkages. The calcium binding motif displayed almost identical chemical shifts in the ^{15}N-HSQC spectra of the SrtA–QALPECG-NH_2 adduct and thioester intermediate. Judging by the chemical shift differences, the structural difference is much greater with respect to free SrtA (Figures S6 and S7).

Next we collected structural restraints for the thioester intermediate. Most of the ^{15}N-HSQC cross-peaks of the thioester intermediate were sufficiently well resolved to enable PCS measurements of samples tagged with a paramagnetic lanthanide ion. SrtA contains a Ca^{2+} binding motif and Ca^{2+} enhances the enzymatic activity.[14] Any paramagnetic lanthanide tag thus needs a higher binding affinity for lanthanide than calcium ions. Moreover, the thiol group of Cys184 must not react with the tag. To address these constraints, we produced the D82C mutant of SrtA and synthesized the new paramagnetic tags T1 and T2 (Figure 2; see the Schemes S2–S5 in the Supporting Information for tag synthesis and ligation with SrtA). T1 reacts with a solvent-exposed thiol group in aqueous solution at pH 7.6, releasing phenylsulfinate as the leaving group. Owing to the bromine atom, it is more reactive than the previously published 4PhSO_2-PyMTA tag.[22] T2 reacts with a protein thiol in a similar manner to 4,4-dithiobisdipicolinic acid, with formation of a disulfide bond.[23] Both tags showed high chemoselectivity towards the thiol group of the cysteine at position 82, and were not reactive towards the side chain of Cys184, as confirmed by chemical shift mapping and MALDI-TOF mass spectra (Figures S8 and S9). The tags show high affinity for lanthanide ions, and this was not compromised by a large excess of Ca^{2+} (up to 20 equivalents).

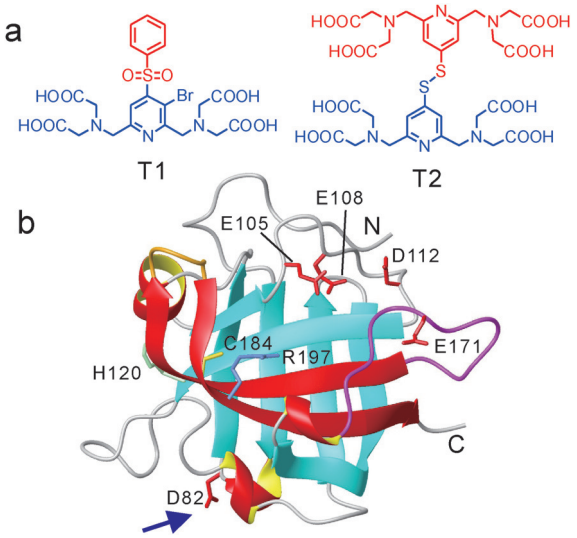

Figure 2. Site-specific labeling of SrtA D82C with a paramagnetic lanthanide tag. a) Chemical structures of the tags T1 and T2 used in the present study. Leaving groups are highlighted in red. b) Ribbon representation of the SrtA structure (PDB ID: 1T2P[15]). The active site and calcium binding site are highlighted by showing the side chains of catalytically important residues (His120, Cys184, and Arg197) and residues involved in calcium binding (Glu105, Glu108, Asp112, Asn114, and Glu171).[21] The strands β7 and β8 are shown in red, the preceding β6/β7 loop in magenta, and the β7/β8 loop in orange. The arrow points at the side chain of Asp82 that was mutated to cysteine for paramagnetic tagging.

To generate the paramagnetically tagged thioester intermediate, solutions of the SrtA D82C-T1 or D82C-T2 adducts were first titrated with lanthanides ions in the presence of calcium, which maintained saturation of the calcium binding site with Ca^{2+} (Figures S10 and S11). Following addition of the QALPETG-NH_2 peptide, paramagnetic cross-peaks were observed for free SrtA D82C-T1 or D82C-T2 and the corresponding thioester intermediates (Figure 3 and Figure S11). PCSs were determined from the ^1H chemical shift differences between the paramagnetic species, generated with Tb^{3+}, Dy^{3+}, or Tm^{3+} ions, and the diamagnetic species, generated with Y^{3+}. Different PCSs were observed for backbone amide protons of the thioester intermediate and free SrtA (Figure 3 and Figures S10–S12).

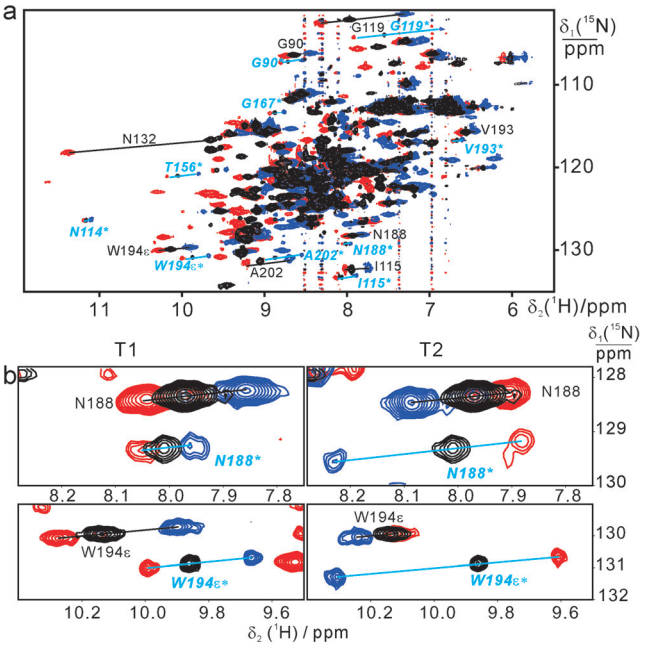

Figure 3. PCSs measured for SrtA D82C labeled with the lanthanide binding tags T1 or T2. Superimpositions of ^{15}N-HSQC spectra measured of 0.15 mM solutions of tagged SrtA D82C in complex with one equivalent of Y^{3+} (black), Tm^{3+} (red), or Tb^{3+} (blue). Selected cross-peaks are labeled with their resonance assignment using dark gray labels and blue labels with a star for the cross-peaks of the free protein and of the thioester intermediate, respectively. a) Spectra of 0.15 mM SrtA D82C with the T1 tag in the presence of 1.0 mM Ca^{2+} and 1.0 mM QALPETG-NH_2. b) Zoom into selected regions of the ^{15}N-HSQC spectra of the thioester intermediate, highlighting differences in the PCSs for the thioester intermediate and the free protein. Left panel: ^{15}N-HSQC spectra of SrtA D82C with the T1 tag. Right panel: ^{15}N-HSQC spectra of SrtA D82C with the T2 tag.

Using the program Numbat,[24] the magnetic susceptibility anisotropy ($\Delta\chi$) tensors of the lanthanide complexes were determined based on PCSs and the crystal structure of free SrtA (PDB ID: 1T2P[15]), using only protein segments with regular secondary structure, for which neither chemical shifts nor PCSs changed significantly between free SrtA and the thioester intermediate. The resulting $\Delta\chi$ tensor parameters are listed in Table S1. Similar $\Delta\chi$ tensors were obtained by using the NMR structure of SrtA (PDB ID: 1IJA,[14] Table S2). The $\Delta\chi$ tensor parameters of the thioester intermediate were similar to those of free SrtA, as expected for structural conservation of much of the protein. Small quality factors indicate that the tags were sufficiently rigid to allow the fitting of each $\Delta\chi$ tensor by a single effective $\Delta\chi$ tensor (Figure S13).[25]

Next we determined the structure of the thioester intermediate. A total of 407 PCSs (262 PCSs for D82C-T1–QALPET, 145 for D82C-T2–QALPET) collected for paramagnetic lanthanide ions (Dy^{3+}, Tb^{3+}, and Tm^{3+} for the T1 tag, and Tb^{3+} and Tm^{3+} for the T2 tag) were used to compute the structure of loop regions in the thioester intermediate using the program Xplor-NIH.[26,27] Figure 4a presents the 20 lowest-energy conformations. The root mean squared deviations of Cα and heavy atoms to the average structure were 0.7 and 1.1 Å, respectively. Starting from the crystal structure of free SrtA and the NMR structure of the disulfide-bond-linked thioester analogue SrtA-LPAT* (PDB ID: 2KID[16]) yielded very similar conformations (Figures S14 and S15, Tables S3 and S4). Compared with the crystal structure of SrtA, the thioester intermediate revealed notable structural changes in the β6/β7 and β7/β8 loops (Figure 4). The residues in these regions are important for catalytic function and were found to undergo conformational exchange in earlier NMR studies of free SrtA.[15,16] In addition, residues in the first helix (α1) and the Ca^{2+} binding motif, including the loop segments β3/β4, β4/α2, and β5/β6, also showed significant structural changes.

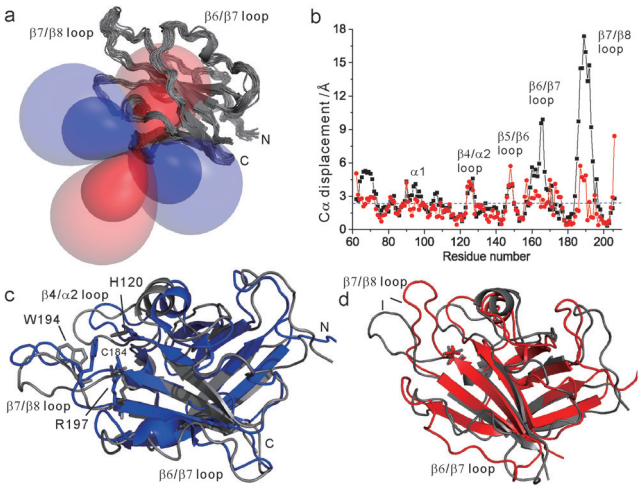

Figure 4. 3D structure of the thioester intermediate defined by PCSs. a) Superimposition of the 20 lowest-energy structures. PCS isosurfaces of the thioester SrtA D82C-T1·Tb^{3+} complex are shown together with the protein structure. The isosurfaces plotted correspond to PCSs of 0.8 and 0.2 ppm (blue), and −0.8 and −0.2 ppm (red). b) Backbone Cα displacement of the lowest-energy structure of the thioester intermediate relative to the crystal structure of free SrtA (black squares; PDB ID: 1T2P[15]) and to the first conformer of the NMR structure of the disulfide linked thioester analogue SrtA-LPAT* (red spheres, PDB ID: 2KID[16]). c) Structure comparison between the thioester intermediate (gray) and SrtA-LPAT* (blue). The side chains of residues 120, 184, and 197, which mark the active site, and of Trp194 are shown in stick representation. Loop regions with significant structural differences are labeled. d) Superimposition of the thioester intermediate (gray) and SrtA with inhibitor (PDB ID: 2MLM[28], red).

The structure of the thioester intermediate most closely resembles the structure of the disulfide-bonded SrtA-LPAT* analogue (Figure 4b,c) and differs significantly from the crystal structure of SrtA with non-covalently bound LPETG peptide (PDB ID: 1T2W[15]), which has almost the same conformation as free SrtA. The β6/β7 and β7/β8 loops in the thioester intermediate also differ significantly from the structure determined for SrtA with an inhibitor linked to Cys184 via a disulfide bond (PDB ID: 2MLM,[28] Figure 4d).

As in the SrtA-LPAT* analogue, Ca^{2+} restricts conformation exchange in the thioester intermediate, as evidenced by the appearance of ^{15}N-HSQC cross-peaks for residues from the β6/β7 loop that are broadened by chemical exchange in free SrtA (Figure 1 and Figure S16).[21] The altered conformation of the β6/β7 loop is interesting, because it forms a connection between the calcium binding site and Cys184 in the active site. The thioester intermediate also displays a more extended conformation of the β7/β8 loop, which facilitates nucleophilic attack on the thioester by an oligo-glycine peptide in the next step of the catalytic cycle.[15]

Despite overall structural similarity, there are also significant differences with respect to the SrtA-LPAT* analogue (Figure S15), which correlate with the chemical shift perturbations (Figures S6 and S7). Most strikingly, the β7/β8 loop differs in the thioester intermediate, including the side chains of Trp194 and His120 (Figure 4b,c). The side chain of Trp194, which resides in the β7/β8 loop, shows a very clear difference in PCSs between free SrtA and the thioester intermediate (Figure 3). This residue contributes to the enzyme function, since four-fold decreased enzymatic activity has been reported for the mutant W194A.[29] The chemical difference between a disulfide bond and a thioester also seems to contribute to structural differences in the β4/α2 loop (Figure 4c), which has been proposed to be involved in the subsequent reaction with oligo-glycine peptides.[16]

To the best of our knowledge, the structure of the short-lived thioester intermediate of SrtA determined here with the help of PCSs presents the first 3D structural view, in solution, of an enzymatic intermediate present only as a minor species under non-equilibrium conditions. The structure determination relied on lanthanide tags of carefully tuned reactivity to avoid modifying Cys184 at the active site. We expect that this strategy will be very useful for the structure analysis of minor protein species that are sufficiently stable to be observable as a separate set of peaks, even if only transiently and with weak intensity.

Acknowledgements

We thank J. T. Wang for the synthesis of the T1 tag. X.C.S. thanks Dr. Charles Schwieters for discussions on the use of Xplor-NIH. Financial support by Major National Scientific Research Projects (2013CB910200 and 2016YFA0501202), National Natural Science Foundation of China (21473095 and 21273121), and the Australian Research Council (DP140100304) is gratefully acknowledged.

Keywords: enzyme catalysis · NMR spectroscopy · protein dynamics · protein structures · transient intermediates

How to cite: *Angew. Chem. Int. Ed.* **2016**, *55*, 13744–13748
Angew. Chem. **2016**, *128*, 13948–13952

[1] a) K. Henzler-Wildman, D. Kern, *Nature* **2007**, *450*, 964–972; b) H. van den Bedem, J. S. Fraser, *Nat. Methods* **2015**, *12*, 307–318; c) D. D. Boehr, D. McElheny, H. J. Dyson, P. E. Wright, *Science* **2006**, *313*, 1638–1642.

[2] a) J. S. Fraser, *Acc. Chem. Res.* **2015**, *48*, 423–430; b) A. G. Palmer, *Acc. Chem. Res.* **2015**, *48*, 457–465; c) P. Hanoian, C. T. Liu, S. Hammes-Schiffer, S. Benkovic, *Acc. Chem. Res.* **2015**, *48*, 482–489.

[3] a) P. L. Ramachandran, J. E. Lovett, P. J. Carl, M. Cammarata, J. H. Lee, Y. O. Jung, H. Ihee, C. R. Timmel, J. J. Van Thor, *J. Am. Chem. Soc.* **2011**, *133*, 9395–9404; b) J. S. Fraser, M. W. Clarkson, S. C. Degnan, R. Erion, D. Kern, T. Alber, *Nature* **2009**, *462*, 669–673; c) P. Schanda, V. Forge, B. Brutscher, *Proc. Natl. Acad. Sci. USA* **2007**, *104*, 11257–11262.

[4] a) C. Tang, J. Iwahara, M. G. Clore, *Nature* **2006**, *444*, 383–386; b) C. Tang, C. D. Schwieters, M. G. Clore, *Nature* **2007**, *449*, 1078–1082.

[5] I. Bertini, A. Giachetti, C. Luchinat, G. Parigi, M. V. Petoukhov, R. Pierattelli, E. Ravera, D. I. Svergun, *J. Am. Chem. Soc.* **2010**, *132*, 13553–13558.

[6] a) P. Neudecker, P. Robustelli, A. Cavalli, P. Walsh, P. Lundström, A. Zarrine-Afsar, S. Sharpe, M. Vendruscolo, L. E. Kay, *Science* **2012**, *336*, 362–366; b) N. L. Fawi, J. Ying, R. Ghirlando, D. A. Torchia, G. M. Clore, *Nature* **2011**, *480*, 268–272; c) P. Vallurupalli, G. Bouvignies, L. E. Kay, *J. Am. Chem. Soc.* **2012**, *134*, 8148–8161; d) D. M. Korzhnev, T. L. Religa, W. Banachewicz, A. R. Fersht, L. E. Kay, *Science* **2010**, *329*, 1312–1316.

[7] a) I. Bertini, C. Luchinat, G. Parigi, *Prog. Nucl. Magn. Reson. Spectrosc.* **2002**, *40*, 249–273; b) G. M. Clore, J. Iwahara, *Chem. Rev.* **2009**, *109*, 4108–4139; c) G. Otting, *Annu. Rev. Biophys.* **2010**, *39*, 387–405; d) M. A. Hass, M. Ubbink, *Curr. Opin. Struct. Biol.* **2014**, *24*, 45–53; e) N. J. Anthis, G. M. Clore, *Q. Rev. Biophys.* **2015**, *48*, 35–116; f) D. M. Korzhnev, L. E. Kay, *Acc. Chem. Res.* **2008**, *41*, 442–451.

[8] L. A. Marraffini, A. C. Dedent, O. Schneewind, *Microbiol. Mol. Biol. Rev.* **2006**, *70*, 192–221.

[9] K. W. Clancy, J. A. Melvin, D. G. McCafferty, *Biopolymers* **2010**, *94*, 385–396.

[10] a) A. H. Chan, J. Wereszczynski, B. R. Amer, S. W. Yi, M. E. Jung, J. A. McCammon, R. T. Clubb, *Chem. Biol. Drug Des.* **2013**, *82*, 418–428; b) S. Cascioferro, D. Raffa, B. Maggio, M. V. Raimondi, D. Schillaci, G. Daidone, *J. Med. Chem.* **2015**, *58*, 9108–9123.

[11] J. R. Scott, T. C. Barnett, *Annu. Rev. Microbiol.* **2006**, *60*, 397–423.

[12] M. W. Popp, H. L. Ploegh, *Angew. Chem. Int. Ed.* **2011**, *50*, 5024–5032; *Angew. Chem.* **2011**, *123*, 5128–5137.

[13] a) J. E. Glasgow, M. L. Salit, J. R. Cochran, *J. Am. Chem. Soc.* **2016**, *138*, 7496–7499; b) H. Hirakawa, S. Ishikawa, T. Nagamune, *Biotechnol. J.* **2015**, *10*, 1487–1492.

[14] U. Ilangovan, T. Ton-That, J. Iwahara, O. Schneewind, R. T. Clubb, *Proc. Natl. Acad. Sci. USA* **2001**, *98*, 6056–6061.

[15] Y. Zong, T. W. Bice, H. Ton-That, O. Schneewind, S. V. Narayana, *J. Biol. Chem.* **2004**, *279*, 31383–31389.

[16] N. Suree, C. K. Liew, V. A. Villareal, W. Thieu, E. A. Fadeev, J. J. Clmens, M. E. Jung, R. T. Clubb, *J. Biol. Chem.* **2009**, *284*, 24465–24477.

[17] S. K. Mazmanian, G. Liu, H. Ton-That, O. Schneewind, *Science* **1999**, *285*, 760–763.

[18] B. A. Frankel, R. G. Kruger, D. E. Robinson, N. L. Kelleher, D. G. McCafferty, *Biochemistry* **2005**, *44*, 11188–11200.

[19] D. C. Cantu, Y. Chen, M. L. Lemons, P. J. Reilly, *Nucleic Acids Res.* **2011**, *39*, D342 – 346.
[20] X. C. Su, T. Huber, N. E. Dixon, G. Otting, *ChemBioChem* **2006**, *7*, 1599 – 1604.
[21] M. T. Naik, N. Suree, U. Ilangovan, C. K. Liew, W. Thieu, D. O. Campbell, J. J. Clemens, M. E. Jung, R. T. Clubb, *J. Biol. Chem.* **2006**, *281*, 1817 – 1826.
[22] Y. Yang, J. T. Wang, Y. Y. Pei, X. C. Su, *Chem. Commun.* **2015**, *51*, 2824 – 2827.
[23] X. Jia, A. Maleckis, T. Huber, G. Otting, *Chem. Eur. J.* **2011**, *17*, 6830 – 6836.
[24] C. Schmitz, M. J. Stanton-Cook, X. C. Su, G. Otting, T. Huber, *J. Biomol. NMR* **2008**, *41*, 179 – 189.
[25] D. Shishmarev, G. Otting, *J. Biomol. NMR* **2013**, *56*, 203 – 216.
[26] C. D. Schwieters, J. J. Kuszewski, N. Tjandra, G. M. Clore, *J. Magn. Reson.* **2003**, *160*, 65 – 73.
[27] C. D. Schwieters, J. J. Kuszewski, G. M. Clore, *Prog. Nucl. Magn. Reson. Spectrosc.* **2006**, *48*, 47 – 62.
[28] D. Zhulenkovs, Z. Rudevica, K. Jaudzems, M. Turks, A. Leonchiks, *Bioorg. Med. Chem.* **2014**, *22*, 5988 – 6003.
[29] H. Ton-That, S. K. Mazmanian, L. Alksne, O. Schneewind, *J. Biol. Chem.* **2002**, *277*, 7447 – 7452.

Received: June 27, 2016
Revised: August 15, 2016
Published online: October 4, 2016

